PV Ramp Rate Smoothing Using Energy Storage to Mitigate Increased Voltage Regulator Tapping

Matthew J. Reno, Matthew Lave, Jimmy E. Quiroz, and Robert J. Broderick

Sandia National Laboratories, Albuquerque, NM, 87185, USA

Abstract — A control algorithm is designed to smooth the variability of PV power output using distributed batteries. The tradeoff between smoothing and battery size is shown. It is also demonstrated that large numbers of highly distributed current, voltage, and irradiance sensors can be utilized to control the distributed storage in a more optimal manner. It is also demonstrated that centralized energy storage control for PV ramp rate smoothing requires very fast communication, typically less than a 15-second update rate. Finally, advanced inverter dynamic reactive current is shown to provide voltage variability smoothing, hence reducing the number of voltage regulator tap changes without energy storage.

Index Terms — energy storage, advanced inverters, distribution system, photovoltaics

I. INTRODUCTION

Solar variability of high penetrations of PV interconnected on the distribution system can cause large fluctuations in the grid voltage. These fluctuations cause more wear and tear on automatic voltage regulation equipment as it tries to keep the voltage within normal operating limits [1]. One major impact is to on-load tap changer or voltage regulators as they change tap positions on their secondary winding to correct the downstream voltage, and more tap changes result in higher O&M costs for the equipment [2].

In this project, energy storage is proposed in order to provide PV ramp rate smoothing to mitigate increased voltage regulator tap changes. An algorithm is developed for controlling a battery to add (or subtract) power to the PV output to smooth the net power injection. The intent is to reduce the high frequency variability of the PV power that occurs during transient cloud shadows, but also to not overwork the battery in order to maintain the optimal power and energy ratings of the battery. The control algorithm also regulates the state of charge (SOC) of the battery and can provide minor energy/load shifting. Two different control strategies are implemented:

1) Only local information is used to control the battery based on the collocated PV system output.
2) Large numbers of highly distributed current, voltage, and irradiance sensors are utilized to control the entire distribution system in a more optimal manner [3, 4].

Scenario (1) is representative of most current solar inverters. But, the portion of residential PV inverters that are communication-enabled has increased recently and is expected to accelerate due to grid support requirements such as California Rule 21.

II. SIMULATION PLATFORM

A real distribution feeder is modeled in OpenDSS to test the storage controls. The circuit, designated Feeder CO1, is a rural 12kV distribution feeder consisting of 2970 medium- and low-voltage buses and 2569 lines servicing 1447 loads through 401 service transformers. A map showing the layout of the feeder topology and the existing voltage regulating devices is shown in Fig. 1. There is one three-phase voltage regulator on the feeder backbone about 6km from the substation and five switching capacitors. The feeder has a peak load of 6.41MW and a minimum load of 1.29MW.

The peak load week of June 27 to July 3rd was selected as the simulation week. Measured substation SCADA data at 1-minute resolution was used to model the load variation. Quasi-static timeseries (QSTS) power flow analysis was performed at 1-second resolution by linearly interpolating the load data to 1-second resolution. The analysis is performed in OpenDSS with all analysis and visualization in MATLAB using the GridPV toolbox [5].
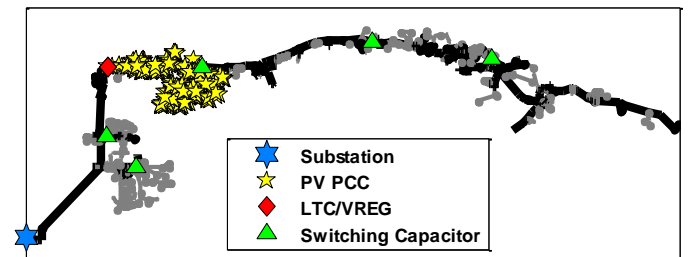

Fig. 1.   Map of Feeder CO1 distributed PV test scenario.

A total of 306 PV systems are simulated all located in the same geographical area in a subdivision, as shown by the clump of yellow stars in Fig. 1. These PV locations are directly downstream of the voltage regulator (red diamond in Fig. 1). By clustering so many PV systems so closely together, this represents a worst case scenario for solar variability with little geographical smoothing. In order to get a very high penetration of PV that causes issues with the number of tap changes on the regulator, each customer in that section is simulated with a PV system that is 2.5 times the size of their individual peak load, with an aggregate total of 2.8 MW of PV. For this section of the feeder, the penetration is 250%, but the penetration is 80% of the load downstream of the regulator and 45% of the total feeder load.

Irradiance measurements at 1-second resolution from an array of 7 irradiance sensors in San Diego, California, were used to generate 91 unique PV power output timeseries profiles, one for each medium-voltage interconnection point (service transformer) on the feeder. For situations with multiple customers connected to a single transformer, each customer was assigned the same irradiance profile. The 91 power profiles were created by first pairing each service transformer with the irradiance sensor network based on their relative latitude. The color coding in Fig. 2 shows the irradiance sensor (open circle) assigned to each transformer (solid dot). Then, the irradiance was time-shifted based on the distance between the (assumed) location of the irradiance sensor and the transformer. The time shift was calculated as the distance divided by the cloud speed, assuming clouds propagate from west to east. Based on a year of cloud speeds at the feeder location, the maximum speed of 24 m/s was simulated in order to demonstrate the worst case PV variability. The resulting time offsets are shown in Fig. 3.
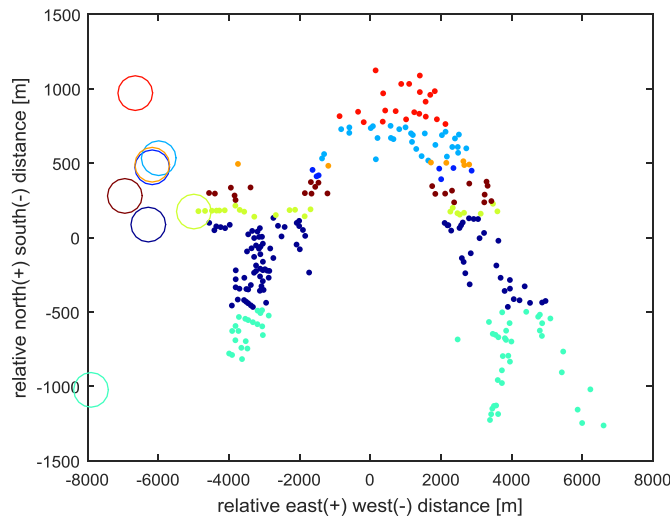

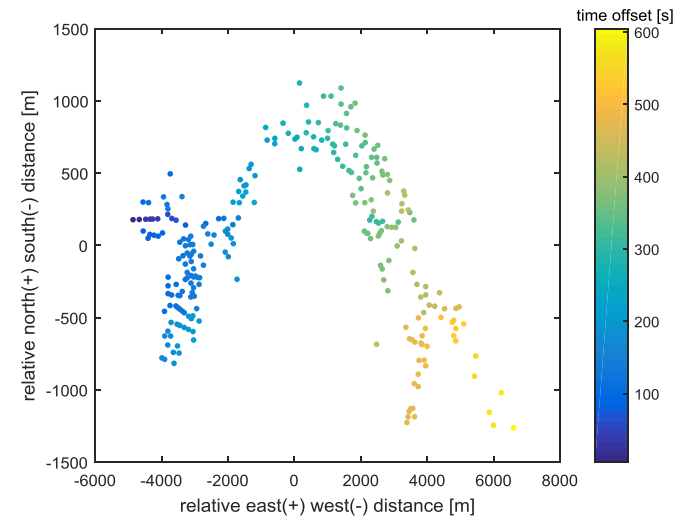Fig. 2.   PV system pairing with irradiance sensors.

Fig. 3.   PV system time offset for 24 m/s cloud speed.

For each transformer, the time-shifted measured irradiance was converted to latitude tilt plane of array (POA) irradiance using the Erbs decomposition and Hay/Davies transposition models [6]. The Sandia Array Performance Model [7] and Sandia Inverter models [8] were used to obtain PV power output from the POA irradiance.

Fig. 4 shows the basecase simulation without any PV and the result of adding the 2.8 MW of distributed PV. While the PV size is significantly less than the peak load downstream of the regulator, because of when the PV is producing, there is regularly reverse current through the regulator.
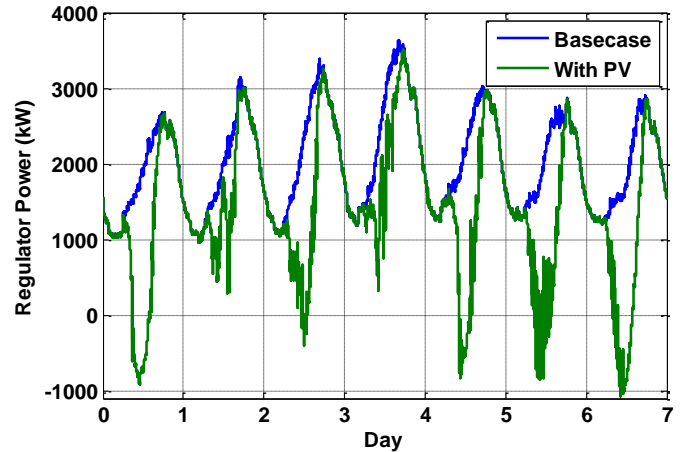

Fig. 4.   The real power transferred through the voltage regulators during the simulation week.

In order to obtain a baseline simulation with a large number of voltage regulator tap changes, many extreme assumptions had to be made. Large utility-scale PV systems can often impact regulator lifetime [9], but for distributed residential PV installations, the geographic smoothing from the distributed layout results in significantly less impact to the voltage regulator [10, 11]. The objective of the research was to investigate the ramp rate smoothing provided by distributed energy storage systems, but there is already naturally significant ramp rate smoothing naturally occurring due to the geographical spread of the residential PV. As previously mentioned, to get as much aggregate solar variability as possible, it was assumed that every customer in a subdivision had a large (2.5 times their peak load) PV system and that the clouds were moving at their maximum speed of 24 m/s. In this way, the number of tap changes during the simulation week increased from 133 to 193, or 45% increase over the baseline, with the 306 PV systems.

A battery energy storage system is co-located with each of the 306 PV systems. The battery systems are modelled after a 550W, 1.2 kWh battery system developed by Enphase. The idea is that since the Enphase AC battery is fully integrated into the Enphase Energy Management System, it could potentially allow for monitoring, communication, and control. The simulated battery systems are assumed to be exactly 50% of the customer's PV size.

The battery control must operate inside the parameters of the battery, so independent of the control logic, the battery cannot output more power than its W rating or charge/discharge outside of the energy storage capabilities. The battery model in OpenDSS is used for the simulation with the default parameters of 90% efficiency converting AC to DC and 90% efficiency converter DC to AC.

III. BATTERY CONTROL ALGORITHM

The battery storage algorithm is implemented using the feedback controls shown in Fig. 5. It is based on previous PV output smoothing work at Sandia [12]. G_1, G_2, and G_3 are the SOC gain, smoothing gain, and curtailment gain, respectively. The purpose of the control system is to balance the tasks of tracking the reference SOC value (SOC_{REF}) with the desired smoothing function. The SOC gain (G_1) charges or discharges the battery in order to return the energy storage back to SOC_{REF}, generally around 0.5, to keep the battery available for smoothing both up and down ramps in PV output. The gain represents how aggressively the battery is returned to the reference state of charge. In a practical application, the gain should be set small enough to allow the smoothing function to take precedence, but large enough to prevent the battery from continuously reaching the SOC limits.

The smoothing signal is based on a time moving average of the PV power, similar to a low pass filter. The control logic requires a value T_W for the length of the moving average time window. A large moving window will create more smoothing, but also requires more energy storage. The third gain (G_3) is solely for curtailment. By increasing this value, the battery system will charge more when the PV power output is high. This has the advantage of reducing reverse power and shifting the PV generation to later in the day when the load is high.

The controls can be done locally or using centralized dispatch. The local control does ramp rate smoothing while only knowing the local PV output. In this case, the PV inverter power output block in Fig. 5 comes directly from the PV system co-located with the energy storage device. For local control, everything is assumed to happen very quickly because there are no communication delays.

The centralized control communicates with all PV/battery systems in order to know the aggregate PV output and dispatch the individual storage devices based on the PV ramps and battery's SOC. In this case, the PV inverter power block in Fig. 5 represents the summation of all PV generation on the feeder at the time of the communication update. For the centralized control, the communication rate is a user input. For example, if the communication rate is 60 seconds, then the central controller will only be updated with the PV systems' power output and batteries' SOC every 60 seconds. The dispatch signal to control the batteries will also happen at the same communication update rate.

For the centralized control, it is important that the control is implemented for each phase separately. The simulation includes the detailed 3-phase unbalanced distribution system model, 3 single-phase voltage regulators, and distributed residential single-phase PV and storage systems. In order to mitigate tap changes for each single-phase voltage regulator, the control diagram Fig. 5 is implemented individually for the three phases by reading the aggregate of the PV output from all customers on the phase and then dispatching the energy storage systems on the phase. It is assumed that it is correctly known which phase each customer is connected. The result is that each phase is receiving a separate dispatch signal and the phase voltage variability is smoothed.
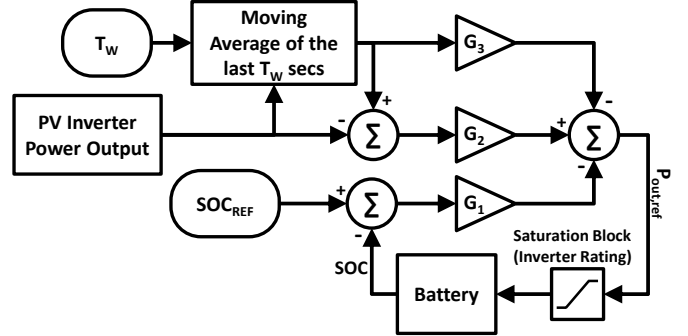

Fig. 5.   Battery control diagram.

An example of the battery smoothing the PV output is shown in Fig. 6 with the battery compensating for any quick changes in PV power injection.
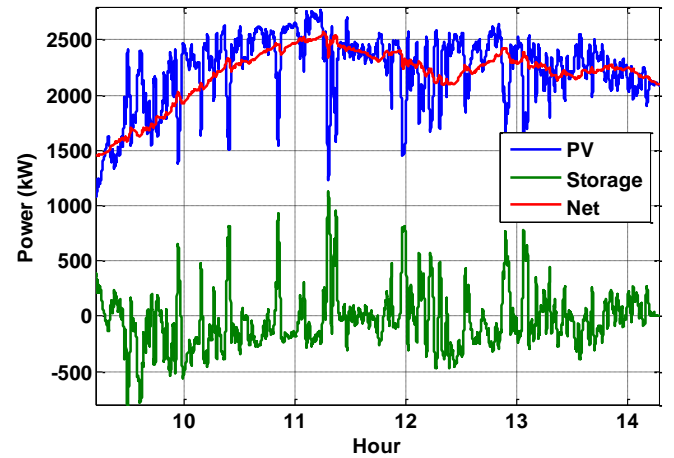

Fig. 6.   Example ramp rate smoothing with energy storage.

Four control types were studied, and their parameters are shown in Table I. The type 2 controls triple the curtailment gain and use much more of the battery to perform the curtailment and shifting of the PV output.

TABLE I. BATTERY CONTROL PARAMETERS.

Control Name	G_1	G_2	G_3	T_W
Local 1	0.7	1.0	0.1	30 min
Local 2	0.5	1.0	0.3	30 min
Central 1	0.7	1.0	0.1	30 min
Central 2	0.5	1.0	0.3	30 min

For this analysis, a fairly simple battery model and control architecture were used to focus on the grid simulations and communication requirements. Other authors have developed improved ramp-rate controls [13] and methods to calculate the required size of the energy storage [14]. No economic modelling was performed [15, 16].

IV. SIMULATION RESULTS

The simulation results for the local control are shown in Fig. 7. As expected, the larger curtailment gain used in the local control 2 results in a lower maximum instantaneous PV output during the day by charging the battery during the middle of the day and injecting the power as the sun is setting in the evening.

Note that the local control battery output does not fully mitigate solar variability during the sharp down ramp at slightly after 11am. This is due to the battery's power rating limiting its output.
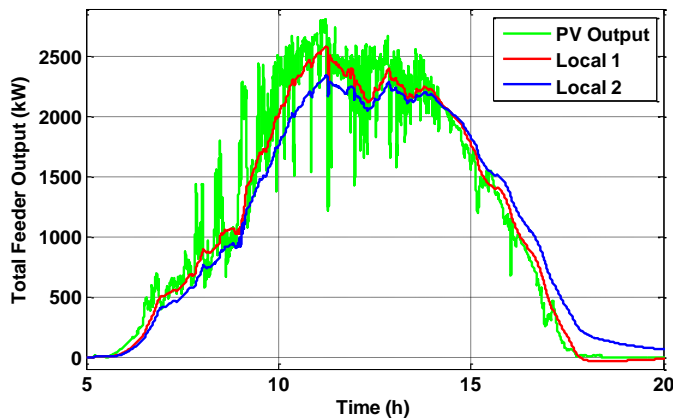

Fig. 7. Aggregate PV and battery power output (kW) for the entire feeder for the local 1 and 2 battery controls.

The central controllers look almost exactly the same at the aggregate feeder level as the local controllers in Fig. 7. There are two main differences between the local and centralized controller. First, there is less energy storage required because sometimes the local controllers can be direction counteracting each other with one charging to smooth a PV up-ramp in power while another discharges to smooth a PV down-ramp in power. Second, the centralized control does slightly better at mitigating the variability slightly after 11am because the controller can command all batteries to help output during the ramp. For both the local and central control, the second control has a larger G_3 curtailment gain, which results in the peak production being slightly lower and the production continuing into later in the evening.

The 1-week QSTS simulation was run for each of the battery control cases. The results are shown in Table II. In addition to the number of tap changes, Table II shows the energy size of the battery required during the simulation. Because the battery size was not constrained during the simulation, the size requirement can be part of the research

question. For example, to mitigate 17 more tap changes, the battery needs to be approximately 4 times larger in the second local and centralized control.

TABLE II. SIMULATION RESULTS.

Control Name	Regulator Tap Changes	Total Required Storage (kWh)
Basecase with PV and No Batteries	193	-
Local 1	154	662
Local 2	137	2710
Central 1	152	629
Central 2	135	2648

The advantages of the central controller can be seen in Table II where the number of tap changes is decreased due to full variability mitigation when individual batteries may have maxed out their power output capabilities. The centralized controller also requires less energy storage capabilities because conflicts between charging and discharging at the same time are removed.

V. COMMUNICATION ANALYSIS

For the central controller, one of the requirements is having fast reliable communication with the PV and battery systems. The results in Table II assume that the centralized controller communicates with all PV/battery systems each second in order to know the aggregate PV output and dispatch the individual storage devices based on the PV ramps and battery's SOC. In order to conserve communication bandwidth, the communication rate might be less frequent. For example, if the communication rate is 60 seconds, then the central controller will only be updated with the PV systems' power output and batteries' SOC every 60 seconds. The dispatch signal to control the batteries will also happen at the same communication update rate. The communication resolution was studied by testing different communication intervals ranging from 1-second to 5-minutes. The results are shown in Fig. 8. Note that there are slightly different results for the number of tap changes depending on when you assume the communication occurs. For example, the 60-second communication resolution 1-week simulation was run four times: with the communication occurring at t=(0,60,120,…), t=(30,90,150,…), t=(15,75,135,…), and t=(45,105,165,…). The average of the four simulations is shown in the thick black line. One interesting result is that there is no decrease in the effectiveness of the centralized controller until the communication rate is slower than 15-second resolution. This corresponds to the Nyquist frequency since the voltage regulator has a 30-second delay. For 60-second or slower communication rates, the resolution is low enough that the centralized controller begins to counteract itself with late actions and performs worse than having no energy storage.
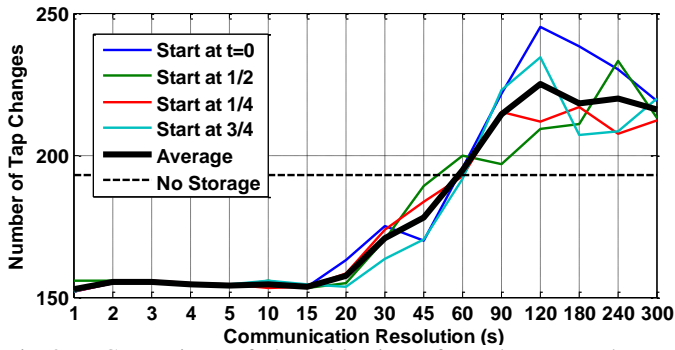
Fig. 8. Comparison of the mitigation of regulator tap changes using centralized control of distributed energy storage systems at different communication rates.

VI. ADVANCED INVERTER CAPABILITIES

While the paper has focused on the ability of energy storage system to mitigate PV variability, there are many functions in current advanced inverters that can also assist in minimizing these impacts [17]. For example, the PV inverters can operate outside maximum power point tracking (MPPT) in order to limit the ramp rate during PV power up-ramps.

At the distribution level, the major impact from solar intermittency is the effect on the grid voltage variability. Advanced inverters can provide some voltage regulation capabilities through reactive power consumption and absorption. The volt-var function provides improvements to the steady-state voltage when the grid voltage is outside the deadband [18]. Additionally, the solar inverter can use an adaptive volt-var curve that substitutes reactive power for real power when fluctuations in the output of the photovoltaic source are experienced [19]. The inverter helps mitigate distribution system voltage fluctuations by adjusting the volt-var curve based on a running historical voltage average.

The adaptive volt-var control has several advantages over other types of controls or energy storage. Compared to energy storage, advanced inverter functionality is fairly inexpensive. There is little additional hardware, and current standards are starting to allow or require certain functionality. While some functions such as volt-var potentially require additional inverter capacity to maintain the desired reactive power output during peak solar production, the adaptive volt-var control has the advantage that it only acts during the transients. As the PV power ramps, it is not at full output so naturally has capacity to generate reactive power. Another advantage of the adaptive control is that it does not consume or generate reactive power under steady-state operations, which might have required the distribution system engineer to redesign the reactive power controls on the feeder. Finally, many advanced inverter controls require very careful tuning to ensure fairness, optimal hosting capacity, and that there is no interaction with existing distribution system equipment [20-22], but the adaptive nature makes the control more robust to system variations and topology changes.

The dynamic reactive current control in the PV inverter model of OpenDSS [23, 24] was used for the simulation with the same 30-minute time-averaging constant. An example of the reactive power output from the PV systems is shown in Fig. 9. When the real power output dips, the grid voltage drops and reactive power is generated to decrease the voltage volatility.
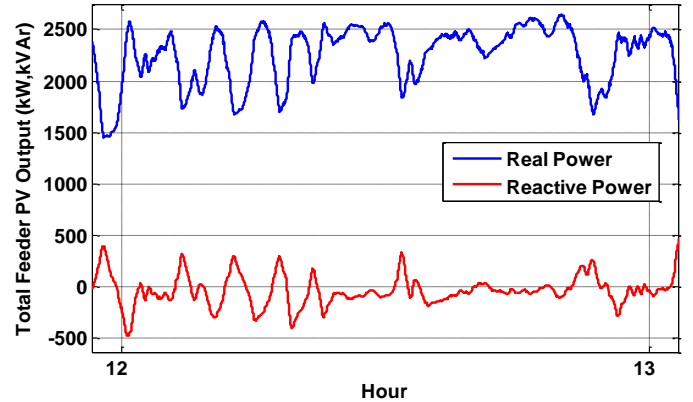

Fig. 9. Total power output from all PV systems when using the dynamic reactive current advanced inverter function.

Using an adaptive volt-var control on the PV advanced inverters, the grid voltage variations are decreased and the number of voltage regulator tap changes is decreased to 159 operations during the simulation week. This is achieved without increasing the PV inverter ratings or installing any energy storage devices.

VII. CONCLUSIONS

A control algorithm was designed to smooth the variability of PV power output using several hundred distributed batteries. The tradeoff between the battery size and the ability to provide smoothing was shown. It was also demonstrated that large numbers of highly distributed current, voltage, and irradiance sensors can be utilized to control the distributed storage in a more optimal manner with an aggregate centralized controller. The communication requirements for the centralized controller were investigated by simulating different communication intervals for how frequently the communication occurred. It was demonstrated that centralized energy storage control for PV ramp rate smoothing requires very fast communication, typically less than a 15-second update rate. Finally, the advanced inverter function of dynamic reactive current was simulated to show the capabilities of the inverter reactive power to provide voltage variability smoothing, hence reducing the number of voltage regulator tap changes without energy storage.

REFERENCES

[1] M. Lave, M. J. Reno, and R. J. Broderick, "Characterizing Local High-Frequency Solar Variability and the Impact to Distribution Studies," *Solar Energy,* 2015.

[2] J. E. Quiroz, M. J. Reno, and R. J. Broderick, "Time Series Simulation of Voltage Regulation Device Control Modes," in *IEEE Photovoltaic Specialists Conference*, 2013.

[3] M. E. Baran and I. M. El-Markabi, "A Multiagent-Based Dispatching Scheme for Distributed Generators for Voltage Support on Distribution Feeders," *IEEE Transactions on Power Systems,* vol. 22, 2007.

[4] H. E. Z. Farag, E. F. El-Saadany, and R. Seethapathy, "A Two Ways Communication-Based Distributed Control for Voltage Regulation in Smart Distribution Feeders," *IEEE Transactions on Smart Grid,* vol. 3, 2012.

[5] M. J. Reno and K. Coogan, "Grid Integrated Distributed PV (GridPV) Version 2," Sandia National Labs SAND2014-20141, 2014.

[6] M. Lave, W. Hayes, A. Pohl, and C. W. Hansen, "Evaluation of Global Horizontal Irradiance to Plane-of-Array Irradiance Models at Locations Across the United States," *IEEE Journal of Photovoltaics,* vol. 5, 2015.

[7] D. L. King, J. A. Kratochvil, and W. E. Boyson, "Photovoltaic array performance model," Sandia National Laboratories SAND2004-3535, 2004.

[8] D. L. King, S. Gonzalez, G. M. Galbraith, and W. E. Boyson, "Performance model for grid-connected photovoltaic inverters," Sandia National Laboratories SAND2007-5036, 2007.

[9] R. J. Broderick, J. E. Quiroz, M. J. Reno, A. Ellis, J. Smith, and R. Dugan, "Time Series Power Flow Analysis for Distribution Connected PV Generation," Sandia National Laboratories SAND2013-0537, 2013.

[10] M. Lave, J. Kleissl, and E. Arias-Castro, "High-frequency irradiance fluctuations and geographic smoothing," *Solar Energy,* vol. 86, 2012.

[11] M. Lave, J. E. Quiroz, M. J. Reno, and R. J. Broderick, "High Temporal Resolution Load Variability Compared to PV Variability," in *IEEE Photovoltaic Specialists Conference*, 2016.

[12] A. Ellis and D. Schoenwald, "PV Output Smoothing with Energy Storage " Sandia National Laboratories SAND2012-1772, 2012.

[13] M. J. E. Alam, K. M. Muttaqi, and D. Sutanto, "A Novel Approach for Ramp-Rate Control of Solar PV Using Energy Storage to Mitigate Output Fluctuations Caused by Cloud Passing," *IEEE Transactions on Energy Conversion,* vol. 29, 2014.

[14] J. Marcos, O. Storkël, L. Marroyo, M. Garcia, and E. Lorenzo, "Storage requirements for PV power ramp-rate control," *Solar Energy,* vol. 99, 2014.

[15] M. Z. Daud, A. Mohamed, and M. A. Hannan, "An improved control method of battery energy storage system for hourly dispatch of photovoltaic power sources," *Energy Conversion and Management,* vol. 73, 2013.

[16] A. Nottrott, J. Kleissl, and B. Washom, "Energy dispatch schedule optimization and cost benefit analysis for grid-connected, photovoltaic-battery storage systems," *Renewable Energy,* vol. 55, 2013.

[17] "Common Functions for Smart Inverters, Version 2," EPRI, Technical Report 1026809, 2012.

[18] M. J. Reno, R. J. Broderick, and S. Grijalva, "Smart Inverter Capabilities for Mitigating Over-Voltage on Distribution Systems with High Penetrations of PV," in *IEEE Photovoltaic Specialists Conference*, Tampa, FL, 2013.

[19] X. Liu, A. M. Cramer, and Y. Liao, "Reactive-power control of photovoltaic inverters for mitigation of short-term distribution-system voltage variability," in *IEEE PES T&D Conference and Exposition*, 2014.

[20] J. Seuss, M. J. Reno, M. Lave, R. J. Broderick, and S. Grijalva, "Multi-Objective Advanced Inverter Controls to Dispatch the Real and Reactive Power of Many Distributed PV Systems," Sandia National Laboratories SAND2016-0023, 2016.

[21] J. Seuss, M. J. Reno, R. J. Broderick, and S. Grijalva, "Analysis of PV Advanced Inverter Functions and Setpoints under Time Series Simulation," Sandia National Laboratories SAND2016-4856, 2016.

[22] M. Rylander, M. J. Reno, J. E. Quiroz, F. Ding, H. Li, R. J. Broderick*, et al.*, "Methods to Determine Recommended Feeder-Wide Advanced Inverter Settings for Improving Distribution System Performance," in *IEEE Photovoltaic Specialist Conference (PVSC)*, 2016.

[23] R. Dugan, W. Sunderman, and B. Seal, "Advanced inverter controls for distributed resources," in *International Conference and Exhibition on Electricity Distribution (CIRED)*, 2013.

[24] W. Sunderman, R. C. Dugan, and J. Smith, "Open source modeling of advanced inverter functions for solar photovoltaic installations," in *IEEE PES T&D Conference and Exposition*, 2014.